Osteoarthritis and Cartilage 24 (2016) 1441–1450

Osteoarthritis and Cartilage

OARSI OSTEOARTHRITIS RESEARCH SOCIETY INTERNATIONAL

A dominant *TRPV4* variant underlies osteochondrodysplasia in Scottish fold cats

B. Gandolfi † **, S. Alamri ‡, W.G. Darby §, B. Adhikari ||, J.C. Lattimer †, R. Malik ¶, C.M. Wade #, L.A. Lyons †, J. Cheng ||, J.F. Bateman ††, P. McIntyre §, S.R. Lamandé ‡ a, B. Haase # * a

† *College of Veterinary Medicine, University of Missouri, Columbia, MO, USA*
‡ *Murdoch Childrens Research Institute, and Department of Paediatrics, University of Melbourne, Royal Children's Hospital, Parkville, Australia*
§ *School of Medical Sciences, RMIT University, Bundoora, Australia*
|| *Computer Science Department, Informatics Institute, C. Bond Life Science Center, University of Missouri, Columbia, MO, USA*
¶ *Centre for Veterinary Education, University of Sydney, Sydney, Australia*
# *Faculty of Veterinary Science, University of Sydney, Sydney, Australia*
†† *Murdoch Childrens Research Institute and Department of Biochemistry and Molecular Biology, University of Melbourne, Parkville, Australia*

ARTICLE INFO

Article history:
Received 15 December 2015
Accepted 25 March 2016

Keywords:
TRPV4
Feline
Bone
Cartilage
Cat
Variant

SUMMARY

Objective: Scottish fold cats, named for their unique ear shape, have a dominantly inherited osteochondrodysplasia involving malformation in the distal forelimbs, distal hindlimbs and tail, and progressive joint destruction. This study aimed to identify the gene and the underlying variant responsible for the osteochondrodysplasia.

Design: DNA samples from 44 Scottish fold and 54 control cats were genotyped using a feline DNA array and a case–control genome-wide association analysis conducted. The gene encoding a calcium permeable ion channel, *transient receptor potential cation channel, subfamily V, member 4* (*TRPV4*) was identified as a candidate within the associated region and sequenced. Stably transfected HEK293 cells were used to compare wild-type and mutant TRPV4 expression, cell surface localisation and responses to activation with a synthetic agonist GSK1016709A, hypo-osmolarity, and protease-activated receptor 2 stimulation.

Results: The dominantly inherited folded ear and osteochondrodysplasia in Scottish fold cats is associated with a p.V342F substitution (c.1024G>T) in *TRPV4*. The change was not found in 648 unaffected cats. Functional analysis in HEK293 cells showed V342F mutant TRPV4 was poorly expressed at the cell surface compared to wild-type TRPV4 and as a consequence the maximum response to a synthetic agonist was reduced. Mutant TRPV4 channels had a higher basal activity and an increased response to hypotonic conditions.

Conclusions: Access to a naturally-occurring *TRPV4* mutation in the Scottish fold cat will allow further functional studies to identify how and why the mutations affect cartilage and bone development.

* Address correspondence and reprint requests to: B. Haase, Faculty of Veterinary Science, University of Sydney, Regimental Drive, B19-305 RMC Gunn, Sydney, 2006 NSW, Australia. Tel: 61-2-8627-0277; Fax: 61-29351-3957.

** Address correspondence and reprint requests to: B. Gandolfi, College of Veterinary Medicine, Department of Veterinary Medicine and Surgery, Vet Med Building, 1600 East Rollins Street, University of Missouri, Columbia, MO, 65201, USA.

E-mail addresses: gandolfib@missouri.edu (B. Gandolfi), sultan.alamri@mcri.edu.au (S. Alamri), bill.darby@rmit.edu.au (W.G. Darby), bap54@mail.missouri.edu (B. Adhikari), lattimerJ@missouri.edu (J.C. Lattimer), richard.malik@sydney.edu.au (R. Malik), claire.wade@sydney.edu.au (C.M. Wade), lyonsla@missouri.edu (L.A. Lyons), chengji@missouri.edu (J. Cheng), john.bateman@mcri.edu.au (J.F. Bateman), peter.mcintyre@rmit.edu.au (P. McIntyre), shireen.lamande@mcri.edu.au (S.R. Lamandé), bianca.waud@sydney.edu.au (B. Haase).

[a] Joint senior authors.

http://dx.doi.org/10.1016/j.joca.2016.03.019

Introduction

Osteochondrodysplasias (or skeletal dysplasias) are a heterogeneous group of disorders caused by structural, metabolic and endocrine defects that compromise cartilage and/or bone growth and give rise to a malformed skeleton[1–3]. Skeletal development is a highly complex process influenced by a vast number of genes and precise tuning of these genes is essential for normal skeletal development. Although individual skeletal dysplasias are rare in humans, research into their pathogenesis has provided valuable insights into bone and cartilage development, as well as more common connective tissue disorders such as osteoarthritis[2,4–6].

One of the biggest challenges in the post-genome era is analysing and dissecting complex and quantitative traits. While such analyses remain a challenge, companion animals provide powerful model populations to study underlying genetic mechanisms. As most dog and cat breeds have been developed within the last 200 years, the remarkable phenotypic and genetic diversity observed today is the result of intense artificial selection. Founder effects at breed creation and subsequent line-breeding have resulted in the unique genetic background of breeds with extensive linkage disequilibrium and long haplotype blocks, compared to human populations[7,8]. While this process has reduced the overall genetic heterogeneity within breeds, it has also enriched alleles with large effects on favourable traits. This population structure is highly advantageous for genome-wide association studies (GWAS) as fewer markers and fewer individuals are required to map even complex traits[9]. An undesirable consequence of the intensive selection for breed-specific traits has been the accumulation of various disease alleles and a high frequency of genetic disorders in many dog and cat breeds. For a remarkable number of these, analogous human genetic disorders are known (http://omia.angis.org.au/home/). Recent advances in feline genomics, including a whole-genome reference sequence[10], and a feline DNA genotyping array[11], have enabled GWAS in cats and allow the cat to be used as a model species to gain insights into the molecular mechanisms underlying human genetic disorders.

Scottish fold cats are characterized by their unique ear shape, caused presumably by reduced resilience of the pinna cartilage. While affected kittens are born with straight ears, the pinnae begin to fold forward at around three to four weeks of age. Based on pedigree information and breeding experiments, the Scottish fold phenotype is inherited as a highly penetrant autosomal dominant trait[12–14]. A congenital degenerative osteochondrodysplasia characterised by malformations in the distal forelimbs, distal hind limbs and tail was initially thought to be restricted to homozygous mutant cats, but was subsequently identified in heterozygous mutant cats[12,15,16]. Based on the initial finding the breeding recommendation for Scottish fold cats is to mate fold-eared cats only with normal eared-cats to avoid producing homozygous mutant cats. Preliminary histologic examinations suggested chondrocyte cell death in articular cartilage, and disturbed maturation of proliferative chondrocytes to hypertrophic chondrocytes in the growth plate[16]. Radiographic examinations suggest defective endochondral ossification resulting in variably reduced length and abnormal shape of the metatarsal and metacarpal bones, accompanied by accelerated degenerative joint disease and progressive peri-articular new bone formation. Interestingly, the age at onset of clinical signs, as well as severity and the progression of the secondary new bone formation is highly variable among affected heterozygous cats. Whether genetic or environmental factors are responsible for the observed phenotypic differences is yet to be determined.

The present study used genetic, computational and *in vitro* strategies to identify the gene underlying the Scottish fold osteochondrodysplasia phenotype. A missense variant in the ***T**ransient **R**eceptor **P**otential **V**anilloid family member **4** gene* (*TRPV4*) is associated with ear folding, abnormal distal appendicular bones and a progressive degenerative joint disorder with different degrees of severity.

Material and methods

Animals and SNP array genotyping

All samples were collected with the permission of the cat's owner, under University of California – Davis institution animal care and use protocol 15933 and with approval of the University of Sydney Animal Ethics Committee (N00/10-2012/3/5837). Cats were sourced from different Scottish fold/Scottish shorthair populations in Europe, Australia and the USA. Radiographs were available from three severely affected Scottish fold cats. One severely affected cat was studied using standard radiography, a helical computerised tomography (CT) and scintigraphy following an intravenous technetium-99m injection to highlight regions with increased bone remodelling. EDTA anti-coagulated blood or non-invasive buccal swab samples were collected from 44 cases (Scottish fold) and 54 controls (22 Scottish shorthairs – strait eared siblings of cats with folded ears, 14 British shorthairs, 13 Selkirk rex and five Persian cats). Genomic DNA was isolated using the DNAeasy Kit (Qiagen, Hilden, Germany) and concentrated using the Genomic DNA Clean & Concentrator Kit (Zymo Research, Irvine, USA) when necessary. Individual genotypes were determined using the Illumina Infinium Feline 63K iSelect DNA array.

Genome-wide association study and fine mapping

Array marker locations were adjusted to the most recent feline genome assembly *Felis catus* 6.2/felCat5[11]. A case–control genome-wide association analysis was performed as previously described[11]. The population substructure within cases and controls was evaluated using a multi-dimensional scaling (MDS) plot with two dimensions and the identical-by-state (IBS) allele-sharing proportion was calculated for each individual using PLINK[17]. Outlier samples and individuals with a proportion of IBS >0.3 were excluded. The GWAS results were adjusted for multiple testing (*-mperm* 100,000) using PLINK[17]. The threshold for genome-wide significance was Bonferroni-adjusted. Linkage disequilibrium and haplotypes in the region from position 23,500,000 to 25,5000,000 of feline chromosome D3 were determined using HAPLOVIEW[18]. The corresponding syntenic region in the mouse genome was searched for potential candidate genes using the Mouse Genome Browser (http://gbrowse.informatics.jax.org/cgi-bin/gb2/gbrowse/mousebuild38/).

PCR and variant analysis

Five cats including two cases (Scottish folds) and three straight-eared controls (one Scottish-shorthair and two domestic shorthairs) were selected for initial variant detection. Primers to amplify the 15 *TRPV4* coding exons (exons 2–16) including the 5′- and 3′-untranslated regions were designed using Primer 3 software (http://biotools.umassmed.edu/bioapps/primer3_www.cgi). Primer sequences are listed in Table S1. PCR products were amplified using the SequalPrep long range PCR kit (Invitrogen, Carlsbad, USA) according to the manufacturer's protocol. An additional primer set was designed for exon 6. PCR products for exon 6 were amplified in 20 μl reactions using AmpliTaq Gold according to the manufacturer's protocol (Applied Biosystems, Foster City, USA). PCR products were treated with shrimp alkaline phosphatase (Roche, Basel, Switzerland) and exonuclease I (New England Biolabs,

Ipswich, USA), then directly sequenced using the PCR primers as well as internal sequencing primers when necessary. Sequencing products were separated using an ABI 3730 capillary sequencer (Applied Biosystems, Foster City, USA), analysed using Sequencher 4.8 (GeneCodes, Ann Arbor, USA) and compared to the feline reference sequence felCat5 September 2011 build. The candidate causative variant was genotyped in all additional Scottish fold and Scottish shorthair samples available (42 Scottish fold and 21 Scottish shorthair). The possible impact of candidate variants on the protein structure was investigated using PolyPhen-2 (http://genetics.bwh.harvard.edu/pph2/).

Population screening

An allele-specific PCR assay was developed to detect the c.1024G>T polymorphism. Cats ($n = 728$) from 40 different populations, including pure-breed and random bred cats, were analysed. Each 25 μl PCR reaction contained template DNA, 1 μM of each primer (forward FAM-AACTACCTGACAGAGAACCCG, the wild-type reverse tgatCAGGTCGTACATCTTGGTGgC and the affected reverse CAGGTCGTACATCTTGGcGAA), 1 × PCR Buffer (Denville Scientific Inc., South Plainfield, USA), 2.5 mM $MgCl_2$, 1.0 mM each dNTP, 0.02 μl DMSO and 1.0 U Choice-Taq DNA polymerase (Denville Scientific, Inc., South Plainfield, USA). Template specificity was increased by incorporating a sequence mismatch in both reverse primers (lower case letter) and the addition of four mismatched bases (lowercase underlined) to create a visually detectable produce size difference. PCR amplicons were visualized on an ABI 3730 DNA Analyzer (Applied Biosystems, Foster City, USA) and analyzed using STRand software[19].

Feline TRPV4 homology modelling

The Protein Data Bank (PDB)[20] was searched for structural templates for the feline TRPV4 protein (XP_003994899.1) using PSI-BLAST[21]. The top ranked human template was used to construct the 3D homology model. The feline wild-type sequence was aligned to the human template using CLUSTAL-W[22] and the 3D homology model of the aligned TRPV4 N-terminal domain (residues 148-397) was illustrated using MODELLER[23].

Expression of normal and mutant TRPV4 in HEK293 cells

Human *TRPV4* cDNA in pcDNA5/FRT/TO (Invitrogen, Carlsbad, USA) has been described previously[24]. Human and cat TRPV4 proteins are the same length and the amino acid sequences are 97% identical. The V342F mutation was introduced using the QuikChange® II XL Site-Directed Mutagenesis Kit (Agilent Technologies) and the entire coding region of the cDNA construct was sequenced to confirm that PCR errors had not been introduced. Flp-In™ T-Rex™-293 cells (Life Technologies, Carlsbad, USA) were transfected using Lipofectamine™ (Life Technologies, Carlsbad, USA) and stably transfected cells selected for five passages with 5 μg/ml blasticidin and 100 μg/ml hygromycin. TRPV4 expression was induced with 1 μg/ml tetracycline for four hours.

Preparation of total cell protein and cell surface biotinylated proteins and immunoblotting

Total cell protein and biotinylated cell surface proteins were isolated and analyzed by immunoblotting as described previously[24] using a rabbit polyclonal TRPV4 antibody (ab39260, Abcam, Cambridge, UK), a monoclonal anti-actin antibody (A3853, Sigma Aldrich, St. Louise, USA), or an anti-transferrin receptor antibody (13-6800, Life Technologies, Carlsbad, USA) and Alexa Fluor®-conjugated secondary antibodies (Life Technologies, Carlsbad, USA). Immunoblots were imaged using a Typhoon™ TRIO Variable Mode Imager (GE Healthcare, Little Chalfont, UK) and bands quantified using ImageQuant TL Software (GE Healthcare, Little Chalfont, UK).

Intracellular calcium measurement

Intracellular calcium ($[Ca^{2+}]_i$) was measured by fluorescence with a FlexStation III (Molecular Devices, Sunnyvale, USA), as described previously[24]. A total of 16,000 cells/well were plated into poly-L-lysine coated 384 well plates, grown for 48 h, TRPV4 expression induced with tetracycline for 4 h, before cells were loaded with 2 μM Fura-2 AM (Molecular Probes, Eugene, USA) for 1 h in the presence of 0.01% pluronic F-127. Loading and experiments were done as described before[24]. Emission intensity was measured at 520 nm in response to the synthetic TRPV4 agonist GSK1016709A, hypo-osmolarity (240 mOsm) and the protease-activated receptor 2 (PAR2) activating peptide SLIGRL (50 μM; Sigma) for 120 s, at intervals of 5.86 s, using excitation wavelengths of 340 and 380 nm. Four independent FlexStation experiments, each with six determinations at each point, were combined and expressed as means ± S.E.M ($n = 4$). Curve fitting and statistics were done using GraphPad Prism 6. One way ANOVA was used for multiple comparisons when there was a single treatment and two-way ANOVA for multiple comparisons when there were multiple treatments or time points.

Results

Radiographic findings

The skeletal phenotype in the Scottish fold cats heterozygous for the missense mutation in exon 6 ranged from mild to severe. Radiographs showed all metatarsal and metacarpal bones are shortened and malformed; some are bent with enlarged proximal and distal epiphyses (Fig. 1, Fig. S1). Intertarsal and tarsometatarsal joint spaces are irregular, indistinct and narrowed (Fig. S1). The corresponding joints in the forelimbs are similarly affected, although generally to a lesser extent. All Scottish fold cats showed peri-articular new bone formation (Fig. 2, Fig. S2), which was along the proximal metatarsal bones, and the distal tarsal bones. The peri-articular new bone appeared smooth in plain radiographs, but the superior resolution of CT and elimination of superimposition demonstrated that new bone was actually laid down irregularly (Fig. 2). The proximal limb joints, long bones of the limbs and the vertebral column were unaffected.

Genome-wide association study

Ninety-eight cats (44 cases and 54 controls) were genotyped on the Illumina Infinium iSelect Feline 63K DNA genotyping array. After quality check 46,203 SNPs, 35 Scottish fold and 32 controls (17 Scottish Shorthair, 8 Selkirk Rex, 3 British Shorthair and 4 Persian) remained for analysis (Fig. S3 (A)–(B)). The analysis identified a significant association on feline chromosome D3, with one SNP at position D3:24,861,228 bp reaching genome-wide significance after correction for multiple testing ($P_{raw} = 4.7 \cdot 10^{-11}$, $P_{genome} = 0.00001$) (Fig. 3). A haplotype block defined in Haploview[18] spanning the interval from D3:24,380,099 bp to D3:25,202,262 bp, harbouring the highest associated SNP, was identified with a frequency of 50% in affected cats (Fig. S4). The haplotype was unique to cases, suggesting association with the dominant trait. Based on the feline genome assembly *F. catus* 6.2/felCat5, this haplotype block contained 23 annotated genes (Table S2). Investigation of the syntenic region in the mouse genome identified *TRPV4* as the strongest positional candidate gene.

Fig. 1. Radiographs of a severely affected Scottish fold cat. (A) Dorsopalmar view of the distal forelimbs. Carpal and carpometacarpal joint spaces are narrowed. Metacarpal bones are shortened. (B) Dorsomedial-plantarolateral oblique view of the distal hind limbs. Metatarsal bones are shortened. A mass of smoothly marginated ankylosing new bone is visible on the plantar aspect of the tibiotarsal, intertarsal and tarsometatarsal joints. Distal intertarsal and tarsometatarsal joint spaces are narrowed.

Fig. 2. Radiological findings in the right distal hindlimb of a severely affected Scottish Fold cat. (A) Lateral radiograph. (B) Three-dimensional volume-rendered computed tomography image. (C) Bone phase scintigraphic image showing the irregularly proliferative area of active bone remodelling (arrows) associated with individual metatarsophalangeal joints.

TRPV4 variant analysis

The *TRPV4* coding sequence (GenBank accession no. XM_003994850.2) was analysed in two cases and three controls. Comparison of all 15 coding exons, including partial intronic sequence, revealed 26 sequence variants (Table I). Eleven variants were located in the coding sequence and five changed the amino acid sequence. Only one exonic variant showed concordance with the folded ear phenotype. Both Scottish fold cats were heterozygous for a missense variant located in exon 6 (c.1024G>T) that was absent in three straight-eared cats. Direct sequencing of 63 cats determined that all 21 Scottish shorthair cats were homozygous for the wild-type allele, two Scottish fold cats were homozygous for the variant allele and 39 Scottish fold cats were heterozygous. A single Scottish fold cat tested homozygous wild-type.

Population screening

Screening of 648 cats representing several breeds and domestic shorthair cats of unknown ear type demonstrated the c.1024G>T substitution was detected only in the Scottish fold breed and was absent in all other populations (Table S3).

Protein domain analysis

The variant leads to a non-conserved p.V342F amino acid substitution and was predicted highly damaging by PolyPhen-2 (score 0.98). Using PSI-BLAST search the human TRPV4 ankyrin repeat domain (PDB code: 4dx1) and the brown rat TRPV1 ion channel protein (PDB code: 3j5p), which both include the cat variant site, were the top matches. Only three residues are different from

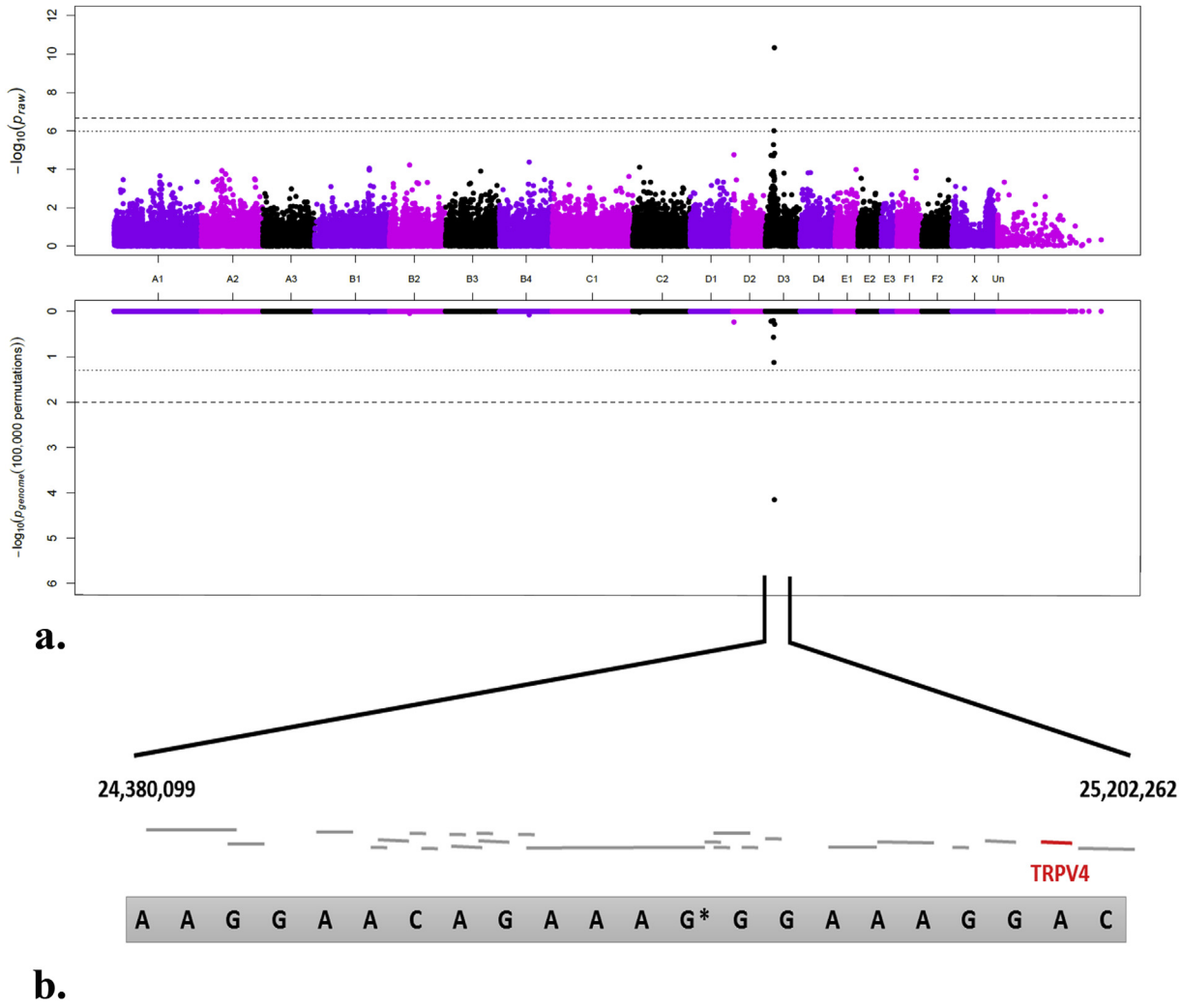

Fig. 3. GWAS identified region associated with osteochondrodysplasia in Scottish fold cats. **a**. A Manhattan plot showing the negative log of the probability of association (*P*-value) between individual markers and osteochondrodysplasia. Markers are shown in alternating colours representing different chromosomes. The upper plot shows P_{raw} values and the lower plot shows values after correction for multiple testing (P_{genome}). Significance of $P \leq 1 \cdot 10^{-8}$ is indicated with a dashed line, a dotted line represents association with $P \leq 1 \cdot 10^{-4}$. **b**. Haplotype unique to cases in the region of association, spanning from position 24,380,099bp to position 25,202,262bp of cat chromosome D3. The asterisk marks the variant significantly associated with osteochondrodysplasia. The haplotype region contains 24 genes (represented by grey lines), including *TRPV4 (indicated in red)*.

human in cat TRPV4 for residues 148 to 397 (Fig. S5). Fig. S5 illustrates the 3D structure of the cat TRPV4 protein region using human TRPV4 as a template.

Functional analysis of TRPV4 wild-type and TRPV4 p.V342F in HEK293 cells

To determine the functional consequences stably transfected HEK293 Flp-In cells expressing either wild-type or mutant TRPV4 were produced. No TRPV4 was detected in untransfected HEK293 cells[24]; however, whole cell lysates from transfected cells contained similar amounts of either wild-type or V342F mutant TRPV4 [Fig. 4(A)–(B)]. In HEK293 cells, TRPV4 has three wild-type isoforms; unglycosylated, a form substituted with a high mannose N-linked oligosaccharide, and a complex N-glycosylated form [Fig. 4(A)]. When compared to wild-type TRPV4, cells expressing V342F mutant TRPV4 contained more of the high mannose form and less of the complex glycosylated form. The localization of TRPV4 was examined using cell surface biotinylation and streptavidin pull-down, followed by immunoblotting to identify and quantitate cell surface proteins. Compared to the wild-type TRPV4, mutant V342F TRPV4 was poorly expressed at the cell surface [Fig. 4(C)–(D)], indicating that the variant altered TRPV4 protein trafficking.

Intracellular calcium imaging was used to evaluate channel activity. A small increase in the constitutive intracellular calcium concentration ($[Ca^{2+}]_i$) was detected in cells expressing wild-type TRPV4 compared to non-transfected cells. Interestingly, $[Ca^{2+}]_i$ was much higher in cells expressing TRPV4 V342F [Fig. 5(A)], indicating that the basal activity of the mutant channels is increased. The response of the channels to the synthetic TRPV4 agonist GSK1016790A showed that intracellular calcium in non-transfected cells was not changed by GSK1016790A [Fig. 5(B)]. By contrast, cells expressing wild-type TRPV4 responded with a dose-dependent increase in $[Ca^{2+}]_i$. Cells expressing V342F mutant TRPV4 also showed a GSK1016790A dose-dependent increase in $[Ca^{2+}]_i$, although the response was reduced compared to wild-type expressing cells and the maximum $[Ca^{2+}]_i$ was significantly lower than in wild-type expressing cells [Fig. 5(B)].

As TRPV4 channels respond to changes in tonicity[25], the response of the wild-type and mutant channels to reduced osmolarity was studied [Fig. 5(C)]. Cells expressing wild-type TRPV4 responded to hypotonic conditions with a rapid increase in $[Ca^{2+}]_i$,

Table I
Sequence variants identified in the cat *TRPV4* gene

Position (genomic DNA)*	Sequence change (cDNA)†	Location	Protein	Scottish fold 1	Scottish fold 2	Scottish shorthair	DSH 1‡	DSH 2
g.25129900	c.25 T>C	Exon 2	Y9H	T/C	T/C	T/C	C/C	T/T
g.25129903	c.28G>A	Exon 2	A10T	G/A	G/A	G/A	G/G	G/G
g.25129908	c.33A>G	Exon 2	Silent	G/G	A/G	A/G	A/A	A/A
g.25129911	c.63T>C	Exon 2	Silent	C/C	T/C	T/C	T/T	T/T
g.25129944	c.69C>T	Exon 2	Silent	C/C	C/C	C/T	0	C/C
g.25130127	c.252C>T	Exon 2	Silent	C/T	C/C	C/C	C/C	C/C
g.25132506	c. 387-69C>T	Intron 2		C/T	C/T	C/T	C/C	C/C
g.25132759	c.559+12A>G	Intron 3		G/A	G/A	G/A	G/G	A/A
g.25136691	c.712+31A>G	Intron 4		A/G	G/G	G/G	A/A	A/A
g.25136847	c.712+166C>G	Intron 4		G/C	G/C	C/C	G/G	0
g.25136866	c.712+185C>T	Intron 4		T/C	T/C	C/C	T/T	0
g.25137266	c.713-152G>A	Intron 4		A/G	A/G	A/G	A/A	A/A
g.25137280	c.713-138C>T	Intron 4		C/T	C/T	C/T	C/C	C/C
g.25138284	c.854-87T>C	Intron 5		C/T	C/T	C/T	C/C	0
g.25138288	c.854-83T>C	Intron 5		C/T	C/T	C/T	C/C	0
g.25138480	c.963A>C	Exon 6	Silent	A/C	A/C	A/C	C/C	A/A
g.25138541	c.1024G>T	Exon 6	**V342F**	**G/T**	**G/T**	G/G	G/G	G/G
g.25138621	c.1104T>C	Exon 6	Silent	T/C	T/C	T/C	T/T	T/T
g.25140888	c.1153-20C>T	Intron 6		C/T	C/C	C/C	C/C	C/C
g.25140902	c. 1153-6G>T	Intron 6		G/T	G/G	G/G	G/G	G/G
g.25142301	c. 1333-17T>C	Intron 7		C/T	C/T	C/C	T/T	T/T
g.25143778	c.1659-66T>C	Intron 10		T/T	T/C	T/T	C/C	0
g.25143830	c. 1659-14C>T	Intron 10		C/C	C/C	C/T	C/C	C/C
g.25144020	c.1824+10C>T	Intron 11		T/C	C/C	C/C	T/T	T/T
g.25146975	c.2041G>A	Exon 13	G681S	G/G	G/A	G/G	G/G	G/G
g.25149751	c.2387G>A	Exon 15	S796N	G/A	G/A	G/A	G/G	G/G

* Numbering refers to chromosome D3 accession ID GCA_000181335.2.
† Numbering refers to accession number XM_003994850.1.
‡ Domestic shorthair. Variations that change the amino acid sequence are highlighted in grey. The heterozygous change leading to a p.V342F amino acid substitution in Scottish fold cats is bolded.

followed by a sustained phase of increased $[Ca^{2+}]_i$. The response of V342F expressing cells to hypotonic conditions was similar; however, the peak response is greater and the increase in $[Ca^{2+}]_i$ during the sustained phase is higher, even when the higher resting $[Ca^{2+}]_i$ is taken into account [Fig. 5(D)].

Another physiological TRPV4 activation mechanism, PAR2 stimulation of TRPV4 signalling, was investigated. Experimentally, PAR2 can be activated by synthetic peptides that mimic the tethered ligand and the response of HEK293 cells expressing wild-type and V342F mutant TRPV4 to the PAR2 activating peptide SLIGRL was tested. As previously reported, untransfected HEK293 cells showed a rapid increase in $[Ca^{2+}]_i$ reflecting release from intracellular stores[26]. In cells expressing wild-type TRPV4 this was followed by a sustained increase in $[Ca^{2+}]_i$ when compared to the transient response seen in untransfected HEK293 cells [Fig. 5(E)]. TRPV4 V342F-expressing cells also had a sustained increase in $[Ca^{2+}]_i$ in response to PAR2 activation, and $[Ca^{2+}]_i$ remained higher than in wild-type expressing cells throughout. However, the baseline adjusted increase in $[Ca^{2+}]_i$ was similar in wild-type and mutant expressing cells indicating that the magnitude of the response was similar [Fig. 5(F)].

Discussion

TRPV4 is expressed in a range of tissues, including chondrocytes, osteoblasts and osteoclasts, where its correct activity is crucial for cell differentiation and tissue homeostasis[5,27,28]. Accordingly, *TRPV4* mutations are responsible for a spectrum of dominantly inherited human skeletal dysplasias, including, autosomal dominant brachyolmia (OMIM 113500), spondylometaphyseal dysplasia Kozlowski type (OMIM 1842522), and metatropic dysplasia (OMIM 156530)[29–31], as well as a premature arthropathy affecting hands and feet, familial digital arthropathy brachydactyly (OMIM 606835)[24]. The TRPV4 skeletal dysplasias show remarkable phenotypic variability and are sometimes accompanied by neurodegenerative disorders[2,24,32–36]. The skeletal dysplasia *TRPV4* mutations that have been examined functionally cause a gain of function and there is evidence that the resulting change in channel conductance determines the severity of the phenotype[37]. While gain of function mutations are responsible for obvious human skeletal malformations, the complete loss of functional TRPV4 has surprisingly little effect on skeletal development in mice[5,28].

The TRPV4 protein has six transmembrane domains and large N- and C-terminal cytoplasmic domains. The N-terminal region contains a single proline-rich domain and six finger-loop forming ankyrin repeat domains[38,39]. The N- and C-terminal cytoplasmic domains play an important role in forming the functional tetrameric cation channel, in addition to anchoring the protein to the cytoskeleton and permitting interactions with other proteins[39–42]. The dominantly inherited folded ear and osteochondrodysplasia in Scottish fold cats is associated with a p.V342F substitution (c.1024G>T) in the fifth ankyrin repeat within the N-terminal cytoplasmic domain (Fig. S5). While the same amino acid substitution has been reported in a human patient with metatropic dysplasia, the mutation has not been functionally characterized[43]. Purified recombinant ankyrin repeat domains containing the V342F mutation have reduced thermal stability compared to wild-type domains and significantly weakened ATP binding even though V342 has no direct interaction with ATP[38]. In wild-type TRPV4, ATP binding leads to a more compact structure made possible by flexibility in finger loop 3 in the ankyrin repeat region which stabilizes the N-terminal domain[38]. ATP sensitises TRPV4 channel activity and so the combination of reduced thermal stability, and altered ATP binding can begin to explain why the p.V342F mutation is pathogenic[44].

To overcome the calcium toxicity that results from extended TRPV4 overexpression, a system was used where TRPV4 is only expressed after induction with tetracycline. This system allows TRPV4 trafficking to the cell surface to be readily compared. TRPV4

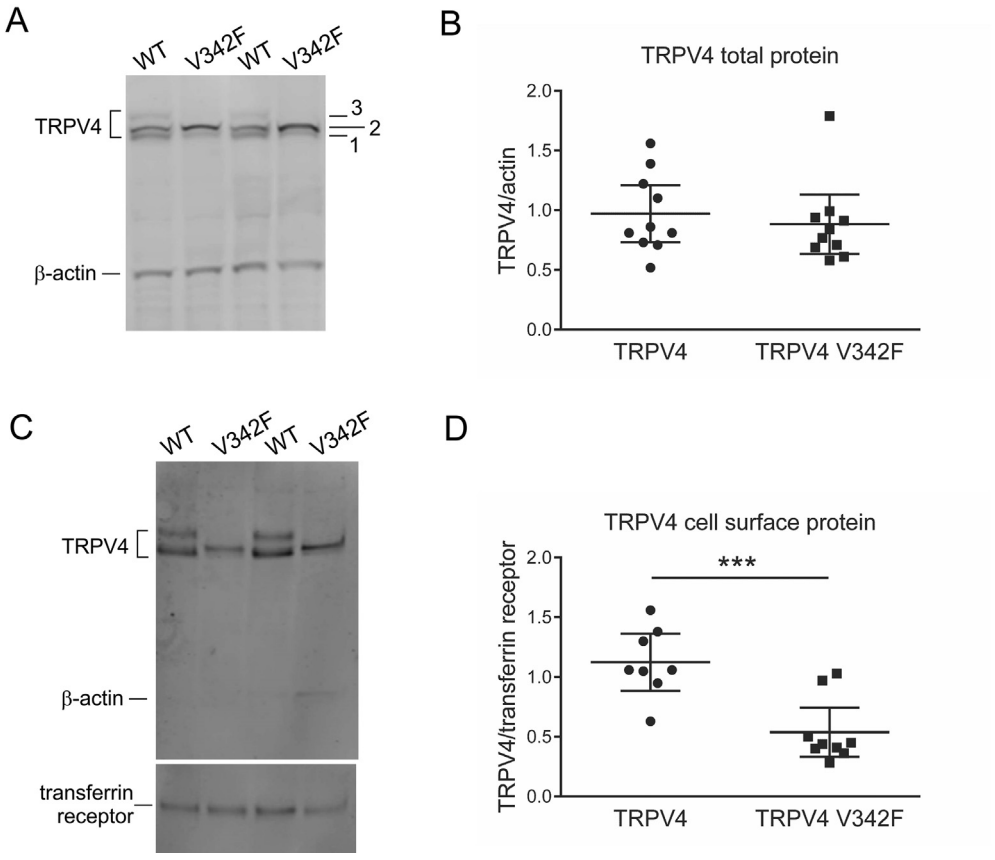

Fig. 4. Wild-type and p.V342F mutant TRPV4 expression in stably transfected HEK293 cells. (A) Immunodetection of TRPV4 and β-actin (loading control) in whole cell lysates. Three TRPV4 isoforms were detected; an unglycosylated form (1), a form substituted with a high mannose N-linked oligosaccharide (2), and a form where the high mannose oligosaccharide had been modified to a complex glycan (3). (B) Quantitating all three TRPV4 bands showed that wild-type and V342F mutant TRPV4 were expressed at similar levels ($P = 0.57$). (C) Cell surface proteins were biotinylated then isolated using streptavidin beads and TRPV4, β-actin and transferrin receptor (loading control) detected by immunoblotting. The absence of a β-actin signal confirms minimal contamination with intracellular proteins. (D) Quantitation of the TRPV4/transferrin receptor ratio shows that V342F mutant TRPV4 is poorly expressed at the cell surface compared to wild-type TRPV4 ($P = 0.0006$). Each point in (B) and (D) is a determination from an individual well. Determinations of multiple wells in two independent experiments are shown. Graphs show mean ± S.E.M. Data sets were compared with the Student's *t* test.

forms a tetramer within the ER and is then trafficked to the cell surface[45]. Two lines of evidence indicate that the V342F mutation impairs channel assembly and trafficking. In whole cell lysates, mutant TRPV4 has less complex N-linked glycosylation and increased high mannose glycosylation, indicating delayed transit from the ER to the Golgi. Secondly, reduced cell surface expression of the mutant channels confirms that intracellular trafficking is disturbed. Thus, the V342F variant likely changes the structure and stability of the N-terminal region, protein interactions critical for tetramer formation and/or stability are compromised and tetramer formation is delayed.

Even though fewer mutant channels were present at the cell surface, in unstimulated conditions the intracellular calcium concentration was higher in cells expressing mutant TRPV4 channels than in wild-type expressing cells. This is consistent with electrophysiology studies that show *TRPV4* skeletal dysplasia mutations increase the channel basal open probabilities[37]. Wild-type and mutant channels responded differently to a range of activating stimuli. The dose response of wild-type and mutant channels to the synthetic agonist GSK1016790A was similar, indicating that the drug was able to efficiently activate both channels. Despite this, the maximum response to GSK1016790A was lower in mutant expressing cells. Since GSK1016790A is thought to drive TRPV4 to its maximum activity[37], the reduced maximum response likely reflects reduced cell surface expression of V342F mutant channels. The V342F mutation did not impact the response of the channels to PAR2 stimulation; however, a gain of function was seen in the response of the mutant channels to hypotonic conditions. V342F expressing cells showed a greater maximum response and had higher sustained intracellular calcium than wild-type expressing cells even after adjusting for the higher basal activity, indicating the mutant channels are more sensitive to hypotonicity than wild-type channels. By contrast, other TRPV4 skeletal dysplasia mutants, D333G, R594H and A716S, showed either reduced or no activation by hypotonic conditions in transiently transfected HEK293 cells[46]. This could reflect different experimental conditions but likely indicates that the downstream pathogenic consequences of TRPV4 mutations are complex and their influence on any individual channel property is only partly informative. Together, these data demonstrate that TRPV4 wild-type and V342F channels behave very differently in response to a synthetic agonist and physiological activation mechanisms, supporting the conclusion that the TRPV4 V342F substitution is pathogenic and causes the bone and joint phenotype in Scottish fold cats.

Interestingly, the skeletal elements that are affected by the TRPV4 V432F mutation are different in humans and cats. The child with the V342F mutation was diagnosed with metatropic dysplasia[43]. While only limited clinical information was reported, the patient had a short trunk and kyphoscoliosis. A review of eleven metatropic dysplasia patients from 20 weeks gestation to 70 years of age found that progressive and severe kyphoscoliosis was a prominent feature[47]. Other common features included platyspondyly,

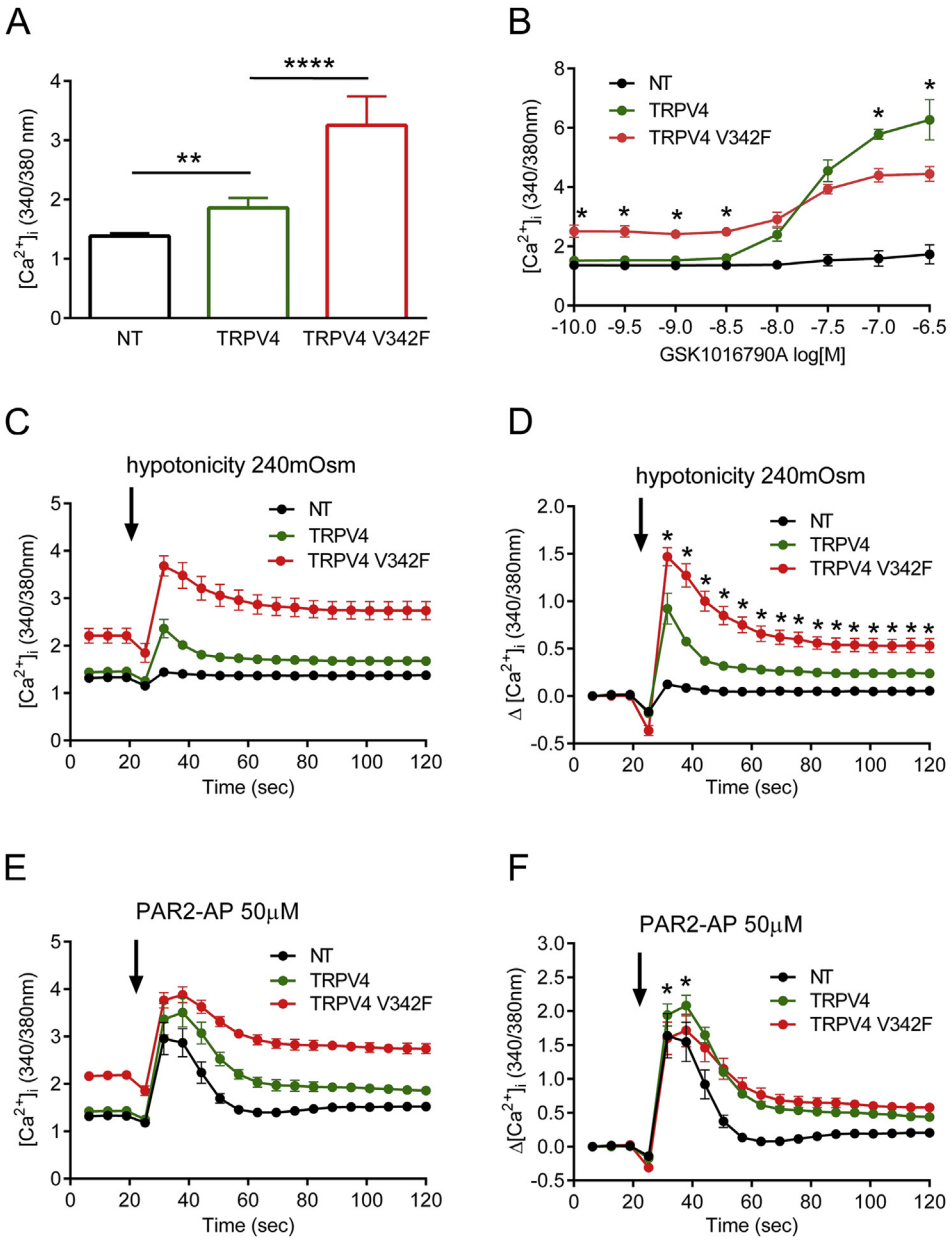

Fig. 5. Intracellular calcium levels in stably transfected HEK293 cells. (A) Constitutive internal fluorescence ratio (**$P < 0.01$, ****$P < 0.0001$, one way ANOVA). (B) Changes in intracellular calcium concentration in response to the synthetic TRPV4 agonist GSK1016790A. Cells expressing wild-type TRPV4 showed a dose dependent increase in intracellular calcium that reached a plateau at higher concentrations. Cells expressing V342F mutant TRPV4 had higher intracellular calcium at low drug doses and reduced responses to GSK1016790A at $10^{-7.0}$ and $10^{-6.5}$ M (*$P < 0.05$, two way ANOVA). (C) Changes in intracellular calcium concentration in response to hypotonicity (240mOsm). The response is characterised by a rapid rise in intracellular calcium followed by a period of lower but sustained increase in intracellular calcium over basal levels. (D) To compare the magnitude of the hypotonicity responses the constitutive fluorescence ratio at time 0 (unstimulated) was subtracted from all other time points. Cells expressing V342F mutant TRPV4 had a higher peak response and maintained a higher response than wild-type expressing cells over the course of the experiment (*$P < 0.05$, two way ANOVA). (E) Changes in intracellular calcium in response to PAR2 activating peptide (PAR2-AP). There is a rapid increase in intracellular calcium reflecting release from internal stores followed by a period of sustained elevated intracellular calcium in cells expressing wild-type and mutant TRPV4. (F) To compare the magnitude of the PAR2 responses the unstimulated fluorescence ratio at time 0 was subtracted from all other time points. When compared in this way wild-type and V342F mutant TRPV4 responded in a similar manner to PAR2 activation although the peak response was higher in mutant expressing cells than wild-type expressing cells (*$P < 0.05$, two way ANOVA). All graphs show mean ± S.E.M.

flaring metaphyseal long bones and short stature. The hands and feet had generalised brachydactyly but no major deformities or abnormal bone growth. By contrast, the distal fore and hindlimbs are severely affected in Scottish fold cats, while the long bones and the spine are relatively spared. The effects of *TRPV4* variants on different skeletal elements could reflect regional species specific differences in biomechanical properties. The biomechanical forces on the spine in a bipedal human are different to those in a quadruped cat[48], and similarly, forces through the feet in a cat that both jumps up and lands from heights will be greater than in most humans. TRPV4 is a mechanosensor in chondrocytes[49]. Our data shows V342F mutant TRPV4 has an elevated response to hypotonicity, a surrogate measure of mechanical stress, compared to wild-type TRPV4 and this altered transduction of mechanical signals likely influences chondrocyte intracellular responses and ultimately, the disease presentation.

Dissecting the complex downstream consequences of *TRPV4* skeletal dysplasia variants will require the appropriate cell types –

chondrocytes, osteoblasts, and osteoclasts – expressing wild-type and mutant *TRPV4* alleles, rather than widely used heterologous cell expression systems. Chondrocytes from patients with *TRPV4* variants are generally inaccessible and until now the only animal models that have been produced are transgenic mice expressing the *Trpv4* V620I or R594H skeletal dysplasia mutations[50,51] under the control of the *Col2a1* promoter. While these mice had a range of skeletal abnormalities similar to those found in human patients, the TRPV4 R594H transgenic mice were generally more severely affected than expected from the intermediate human spondylometaphyseal dysplasia Kozlowski type that results from the R594H mutation[50]. This failure to accurately reproduce the human phenotype could stem from both inappropriately high TRPV4 expression in cartilage and inappropriate expression in the hypertrophic region of the growth plate cartilage. While the *Col2a1* promoter is active in the hypertrophic region and the TRPV4 transgene product was expressed there[50,51], TRPV4 is not normally expressed in these terminally differentiated chondrocytes[24]. Access to a naturally-occurring *TRPV4* variant in a large animal model opens the door to further functional studies concerning how and why the mutation affects cartilage and bone development, and the pathogenesis of accelerated osteoarthritis.

Author contribution

BG, SRL, JFB, LAL, PM and BH designed research. BG, SA, BD, BA, JCL, SRL and BH performed research. LAL, RM JCL contributed case material, radiographs and reagents. BG, SA, BD, CMW, PM, RM, SRL and BH analysed data. SRL, BG and BH wrote the paper. All authors read and approved the submitted manuscript version.

Competing interest statement

The authors have declared that they have no competing interests.

Role of the funding source

This study was supported by the Cat Health Network (D12FE-514), the Morris Animal Foundation (D12FE-021), the National Health and Medical Research Council of Australia (1025715 and 1043837), the Victorian Government's Operational Infrastructure Support Program, previously by the National Institutes of Health National Center for Research Resources R24 RR016094 and is currently supported by the Office of Research Infrastructure Programs/OD R24OD010928 and the University of Missouri – Columbia Gilbreath-McLorn Endowment (LAL). Richard Malik is supported by the Valentine Charlton Bequest. Study sponsors played no role in the study design, collection, analysis or interpretation of data.

Acknowledgements

The authors would like to thank all cat owners and breeders for their support. Sarah Davies contributed to radiographic interpretation and nomenclature.

Supplementary data

Supplementary data related to this article can be found at http://dx.doi.org/10.1016/j.joca.2016.03.019.

References

1. Groza T, Hunter J, Zankl A. The Bone Dysplasia Ontology: integrating genotype and phenotype information in the skeletal dysplasia domain. BMC Bioinforma 2012;13:50.
2. Krakow D, Rimoin DL. The skeletal dysplasias. Genet Med 2010;12:327–41.
3. Hall CM. International nosology and classification of constitutional disorders of bone. Am J Med Genet 2001;2002(113):65–77.
4. Superti-Furga A, Bonafe L, Rimoin DL. Molecular-pathogenetic classification of genetic disorders of the skeleton. Am J Med Genet 2001;106:282–93.
5. Clark AL, Votta BJ, Kumar S, Liedtke W, Guilak F. Chondroprotective role of the osmotically sensitive ion channel transient receptor potential vanilloid 4: age- and sex-dependent progression of osteoarthritis in Trpv4-deficient mice. Arthritis Rheum 2010;62:2973–83.
6. Rukavina I, Mortier G, Van Laer L, Frkovic M, Dapic T, Jelusic M. Mutation in the type II collagen gene (COL2AI) as a cause of primary osteoarthritis associated with mild spondyloepiphyseal involvement. Semin Arthritis Rheum 2014;44:101–4.
7. Karlsson EK, Lindblad-Toh K. Leader of the pack: gene mapping in dogs and other model organisms. Nat Rev Genet 2008;9:713–25.
8. Alhaddad H, Khan R, Grahn RA, Gandolfi B, Mullikin JC, Cole SA, *et al*. Extent of linkage disequilibrium in the domestic cat, Felis silvestris catus, and its breeds. PLoS One 2013;8:e53537.
9. Gandolfi B, Gruffydd-Jones TJ, Malik R, Cortes A, Jones BR, Helps CR, *et al*. First WNK4-hypokalemia animal model identified by genome-wide association in Burmese cats. PLoS One 2012;7:e53173.
10. Montague MJ, Li G, Gandolfi B, Khan R, Aken BL, Searle SM, *et al*. Comparative analysis of the domestic cat genome reveals genetic signatures underlying feline biology and domestication. Proc Natl Acad Sci USA 2014;111:17230–5.
11. Alhaddad H, Gandolfi B, Grahn RA, Rah HC, Peterson CB, Maggs DJ, *et al*. Genome-wide association and linkage analyses localize a progressive retinal atrophy locus in Persian cats. Mamm Genome 2014;25:354–62.
12. Takanosu M, Takanosu T, Suzuki H, Suzuki K. Incomplete dominant osteochondrodysplasia in heterozygous Scottish Fold cats. J Small Anim Pract 2008;49:197–9.
13. Todd NB. Folded-ear cats: further observations. Carn Genet News 1972;2:64–5.
14. Dyte CE, Turner P. Further data on folded-ear cats. Carn Genet News 1973;2:112.
15. Jackson OF. Congenital bone lesion in cats with folded-ears. Bull Feline Advis Bureau 1975;14:2–4.
16. Malik R, Allan GS, Howlett CR, Thompson DE, James G, McWhirter C, *et al*. Osteochondrodysplasia in Scottish Fold cats. Aust Vet J 1999;77:85–92.
17. Purcell S, Neale B, Todd-Brown K, Thomas L, Ferreira MA, Bender D, *et al*. PLINK: a tool set for whole-genome association and population-based linkage analyses. Am J Hum Genet 2007;81:559–75.
18. Barrett JC, Fry B, Maller J, Daly MJ. Haploview: analysis and visualization of LD and haplotype maps. Bioinformatics 2005;21:263–5.
19. Toonen RJ, Hughes S. Increased throughput for fragment analysis on an ABI PRISM 377 automated sequencer using a membrane comb and STRand software. Biotechniques 2001;31:1320–4.
20. Berman H, Henrick K, Nakamura H. Announcing the worldwide protein Data Bank. Nat Struct Biol 2003;10:980.
21. Altschul SF, Madden TL, Schaffer AA, Zhang J, Zhang Z, Miller W, *et al*. Gapped BLAST and PSI-BLAST: a new generation of protein database search programs. Nucleic Acids Res 1997;25:3389–402.
22. Larkin MA, Blackshields G, Brown NP, Chenna R, McGettigan PA, McWilliam H, *et al*. Clustal W and Clustal X version 2.0. Bioinformatics 2007;23:2947–8.

23. Eswar N, Eramian D, Webb B, Shen MY, Sali A. Protein structure modeling with MODELLER. Methods Mol Biol 2008;426:145–59.
24. Lamande SR, Yuan Y, Gresshoff IL, Rowley L, Belluoccio D, Kaluarachchi K, *et al*. Mutations in TRPV4 cause an inherited arthropathy of hands and feet. Nat Genet 2011;43:1142–6.
25. Alessandri-Haber N, Yeh JJ, Boyd AE, Parada CA, Chen X, Reichling DB, *et al*. Hypotonicity induces TRPV4-mediated nociception in rat. Neuron 2003;39:497–511.
26. Grace MS, Lieu T, Darby B, Abogadie FC, Veldhuis N, Bunnett NW, *et al*. The tyrosine kinase inhibitor bafetinib inhibits PAR2-induced activation of TRPV4 channels in vitro and pain in vivo. Br J Pharmacol 2014;171:3881–94.
27. Muramatsu S, Wakabayashi M, Ohno T, Amano K, Ooishi R, Sugahara T, *et al*. Functional gene screening system identified TRPV4 as a regulator of chondrogenic differentiation. J Biol Chem 2007;282:32158–67.
28. Masuyama R, Vriens J, Voets T, Karashima Y, Owsianik G, Vennekens R, *et al*. TRPV4-mediated calcium influx regulates terminal differentiation of osteoclasts. Cell Metab 2008;8:257–65.
29. Nilius B, Voets T. The puzzle of TRPV4 channelopathies. EMBO Rep 2013;14:152–63.
30. Verma P, Kumar A, Goswami C. TRPV4-mediated channelopathies. Channels (Austin) 2010;4:319–28.
31. Andreucci E, Aftimos S, Alcausin M, Haan E, Hunter W, Kannu P, *et al*. TRPV4 related skeletal dysplasias: a phenotypic spectrum highlighted byclinical, radiographic, and molecular studies in 21 new families. Orphanet J Rare Dis 2011;6:37.
32. Zimon M, Baets J, Auer-Grumbach M, Berciano J, Garcia A, Lopez-Laso E, *et al*. Dominant mutations in the cation channel gene transient receptor potential vanilloid 4 cause an unusual spectrum of neuropathies. Brain 2010;133:1798–809.
33. Camacho N, Krakow D, Johnykutty S, Katzman PJ, Pepkowitz S, Vriens J, *et al*. Dominant TRPV4 mutations in nonlethal and lethal metatropic dysplasia. Am J Med Genet A 2010;152A:1169–77.
34. Nishimura G, Dai J, Lausch E, Unger S, Megarbane A, Kitoh H, *et al*. Spondylo-epiphyseal dysplasia, Maroteaux type (pseudo-Morquio syndrome type 2), and parastremmatic dysplasia are caused by TRPV4 mutations. Am J Med Genet A 2010;152A:1443–9.
35. Rock MJ, Prenen J, Funari VA, Funari TL, Merriman B, Nelson SF, *et al*. Gain-of-function mutations in TRPV4 cause autosomal dominant brachyolmia. Nat Genet 2008;40:999–1003.
36. Nilius B, Owsianik G. Channelopathies converge on TRPV4. Nat Genet 2010;42:98–100.
37. Loukin S, Su Z, Kung C. Increased basal activity is a key determinant in the severity of human skeletal dysplasia caused by TRPV4 mutations. PLoS One 2011;6:e19533.
38. Inada H, Procko E, Sotomayor M, Gaudet R. Structural and biochemical consequences of disease-causing mutations in the ankyrin repeat domain of the human TRPV4 channel. Biochemistry 2012;51:6195–206.
39. Clapham DE, Runnels LW, Strubing C. The TRP ion channel family. Nat Rev Neurosci 2001;2:387–96.
40. Montell C, Birnbaumer L, Flockerzi V. The TRP channels, a remarkably functional family. Cell 2002;108:595–8.
41. Arniges M, Fernandez-Fernandez JM, Albrecht N, Schaefer M, Valverde MA. Human TRPV4 channel splice variants revealed a key role of ankyrin domains in multimerization and trafficking. J Biol Chem 2006;281:1580–6.
42. Lei L, Cao X, Yang F, Shi DJ, Tang YQ, Zheng J, *et al*. A TRPV4 channel C-terminal folding recognition domain critical for trafficking and function. J Biol Chem 2013;288:10427–39.
43. Dai J, Kim OH, Cho TJ, Schmidt-Rimpler M, Tonoki H, Takikawa K, *et al*. Novel and recurrent TRPV4 mutations and their association with distinct phenotypes within the TRPV4 dysplasia family. J Med Genet 2010;47:704–9.
44. Phelps CB, Wang RR, Choo SS, Gaudet R. Differential regulation of TRPV1, TRPV3, and TRPV4 sensitivity through a conserved binding site on the ankyrin repeat domain. J Biol Chem 2010;285:731–40.
45. Hellwig N, Albrecht N, Harteneck C, Schultz G, Schaefer M. Homo- and heteromeric assembly of TRPV channel subunits. J Cell Sci 2005;118:917–28.
46. Krakow D, Vriens J, Camacho N, Luong P, Deixler H, Funari TL, *et al*. Mutations in the gene encoding the calcium-permeable ion channel TRPV4 produce spondylometaphyseal dysplasia, Kozlowski type and metatropic dysplasia. Am J Hum Genet 2009;84:307–15.
47. Kannu P, Aftimos S, Mayne V, Donnan L, Savarirayan R. Metatropic dysplasia: clinical and radiographic findings in 11 patients demonstrating long-term natural history. Am J Med Genet A 2007;143A:2512–22.
48. Ianuzzi A, Pickar JG, Khalsa PS. Determination of torque-limits for human and cat lumbar spine specimens during displacement-controlled physiological motions. Spine J 2009;9:77–86.
49. O'Conor CJ, Leddy HA, Benefield HC, Liedtke WB, Guilak F. TRPV4-mediated mechanotransduction regulates the metabolic response of chondrocytes to dynamic loading. Proc Natl Acad Sci U S A 2014;111:1316–21.
50. Weinstein MM, Tompson SW, Chen Y, Lee B, Cohn DH. Mice expressing mutant Trpv4 recapitulate the human TRPV4 disorders. J Bone Min Res 2014;29:1815–22.
51. Leddy HA, McNulty AL, Lee SH, Rothfusz NE, Gloss B, Kirby ML, *et al*. Follistatin in chondrocytes: the link between TRPV4 channelopathies and skeletal malformations. FASEB J 2014;28:2525–37.